HHS Public Access

Author manuscript

FASEB J. Author manuscript; available in PMC 2025 January 22.

Published in final edited form as:

FASEB J. 2020 June ; 34(6): 7915–7926. doi:10.1096/fj.201902179R.

Modulation of radiation-induced damage of human glomerular endothelial cells by SMPDL3B

Alaa Abou Daher[1], **Marina Francis**[1], **Patrick Azzam**[1], **Anis Ahmad**[2], **Assaad A. Eid**[1], **Alessia Fornoni**[3], **Brian Marples**[2], **Youssef H. Zeidan**[2,4]

[1]Faculty of Medicine, American University of Beirut, Beirut, Lebanon

[2]Department of Radiation Oncology, Miller School of Medicine, Sylvester Cancer Center, University of Miami, Miami, FL, USA

[3]Division of Nephrology, Department of Medicine, Peggy, Harold Katz Family Division of Nephrology and Hypertension, University of Miami, Miami, FL, USA

[4]Department of Radiation Oncology, American University of Beirut, Beirut, Lebanon

Abstract

The intracellular molecular pathways involved in radiation-induced nephropathy are still poorly understood. Glomerular endothelial cells are key components of the structure and function of the glomerular filtration barrier but little is known about the mechanisms implicated in their injury and repair. The current study establishes the response of immortalized human glomerular endothelial cells (GEnC) to ionizing radiation (IR). We investigated the role of sphingolipids and the lipid-modifying enzyme sphingomyelin phosphodiesterase acid-like 3b (SMPDL3b) in radiation-induced GEnC damage. After delivering a single dose of radiation, long and very-long-chain ceramide species, and the expression levels of SMPDL3b were elevated. In contrast, levels of ceramide-1-phosphate (C1P) dropped in a time-dependent manner although mRNA and protein levels of ceramide kinase (CERK) remained stable. Treatment with C1P or knocking down SMPDL3b partially restored cell survival and conferred radioprotection. We also report a novel role for the NADPH oxidase enzymes (NOXs), namely NOX1, and NOX-derived reactive oxygen species (ROS) in radiation-induced GEnC damage. Subjecting cultured endothelial cells to radiation was associated with increased NOX activity and superoxide anion generation. Silencing NOX1 using NOX1-specific siRNA mitigated radiation-induced oxidative stress and cellular injury. In addition, we report a novel connection between NOX and SMPDL3b. Treatment with the NOX inhibitor, GKT, decreased radiation-induced cellular injury and restored SMPDL3b basal levels of expression. Our findings indicate the importance of SMPDL3b as a potential therapeutic target in radiation-induced kidney damage.

Correspondence: Youssef H. Zeidan, Department of Radiation Oncology, Medical Center, American University of Beirut, PO Box 11-0236, Riad El Solh 1107 2020, Beirut, Lebanon. yz09@aub.edu.lb.

AUTHOR CONTRIBUTIONS

Y. Zeidan, A. Fornoni, A.A. Eid, and B. Marples designed the research; A. Ahmad, Y. Zeidan, and A. Abou Daher analyzed the data; A. Ahmad, A. Abou Daher, P. Azzam, and M. Francis performed the research; A. Abou Daher and Y. Zeidan wrote the paper; and all authors contributed to editing the paper.

DISCLOSURES

Alessia Fornoni is consultant for Hoffman-La Roche, Alexion, and Mesoblast on subject matters that are unrelated to this publication. The authors declare no conflict of interest.

Keywords

cancer; ceramide; glomerular endothelial cells; nephropathy; radioprotection; reactive oxygen species; SMPDL3b; sphingolipids

1 | INTRODUCTION

The kidneys are radiosensitive tissues that often suffer from collateral damage during the management of abdominal or paraspinal tumors with radiotherapy (RT).[1,2] Radiation induces cellular toxicity in almost all constituents of the human kidney, including the blood vessels and the endothelial cells lining them, the glomeruli, and the tubules and their interstitium.[3] Excessive irradiation of the kidneys eventually results in radiation nephropathy, a gradual irreversible damage to the renal system associated with renal failure.[4] The clinical manifestations of radiation nephropathy depend on the volume and the dose of radiation and the duration of the treatment. Radiation nephropathy commences as an acute phase of proteinuria followed by decreased glomerular filtration rate (GFR), renal tissue atrophy, and progression into end-stage renal disease (ESRD).[5] ESRD requires renal replacement therapy such as dialysis and transplantation.

There has been extensive research in the past decade conducted by our laboratory and others in an attempt to decipher the molecular mechanisms involved in the development of nephropathies.[6–9] Prior work identified the glomerulus to be a key player in renal failure.[10] Among the different glomerular cells, podocytes have received considerable attention during the development of various nephrotic and nephritic syndromes.[7] However, other components of the glomerular filtration barrier (GFB), namely the human glomerular endothelial cells (GEnC), remain poorly investigated, despite being constantly recognized as key players in primary and secondary glomerular diseases.

The pathogenesis of radiation-induced tissue injury, including the renal tissues, involves depletion of organ-specific progenitor stem cells and damage to the microvascular endothelial cells of the capillaries supplying these organs.[11] Glomerular endothelial cells are specialized cells lining the glomerular capillary tufts. Despite the strategic location and unique features of these cells, they have been poorly studied due to the complexity of their isolation and maintenance in culture.[12] The current work explores for the first time the effect of RT on the kidney glomerulus with a particular focus on the glomerular endothelial cells.

Numerous studies conducted by our group highlighted the importance of sphingolipids in preserving normal renal function.[6,13–16] The sphingomyelin phosphodiesterase acid-like 3b (SMPDL3b) enzyme is of particular interest to our work. Although the enzymatic activity of SMPDL3b is not well-established yet, evidence pinpoints that SMPDL3b is located on the lipid rafts of podocytes and is involved in regulating ceramide and ceramide-1-phosphate (C1P) levels.[17–18] Podocyte-specific expression of SMPDL3b has been shown to play a role in focal segmental glomerulosclerosis (FSGS) and to facilitate cytoskeletal remodeling and cell migration.[17,19] In the context of RT, recent work from our group has established the role of SMPDL3b in radiation-induced podocytopathy.[6,17] Ionizing radiation (IR) was shown to trigger podocyte-specific loss of SMPDL3b and induce changes in the sphingolipidomic

profile which correlate with cell injury. Podocytes which overexpress SMPDL3b had a higher degree of radioresistance.[6]

The goal of the current project is to investigate the role of SMPDL3b and sphingolipids in the radiation-induced injury of GEnC. We hereby show that GEnC upregulate SMPDL3b in response to radiation. This upregulation is shown to be mediated by a mechanism involving NADPH oxidase (NOX) enzymes and reactive oxygen species (ROS). Finally, we show that exogenous C1P administration, NOX inhibition, or knockout of SMPDL3b partially reverse radiation-induced endothelial cell injury.

2 | MATERIALS AND METHODS

2.1 | Materials

Endothelial Cell Growth Medium-2 (EGM-2) was purchased from Lonza (Basel, Switzerland). Phosphate-buffered saline (PBS), penicillin-streptomycin, bovine serum albumin, RIPA lysis and extraction buffer, and MTT Cell Proliferation Assay kit were purchased from Thermo Fisher Scientific (Waltham, MA, USA). Fetal bovine serum (FBS) was from Sigma-Aldrich (St. Louis, Missouri, USA). In addition, anti-CERK antibody was obtained from Sigma-Aldrich (St. Louis, Missouri, USA), whereas anti-caspase 9 antibody was obtained from Cell Signaling Technology (Danvers, MA, USA). Anti-SMPDL3b was obtained from GenWay (San Diego, CA, USA). DAPI (49,6-diamidino-2-phenylindole, dihydro-chloride) and DHE (dihydroethidium) were obtained from Thermo Fischer Scientific. Horseradish peroxidase (HRP)-conjugated anti-rabbit was from Promega (Madison, WI, USA). HRP-conjugated anti-mouse IgG, monoclonal anti-GAPDH antibody, protease, and phosphatase inhibitor cocktails were purchased from Calbiochem (San Diego, CA, USA). RNA extraction mini kit was from Qiagen (Valencia, CA, USA). NOX-1, NOX-4, and SMPDL3b forward and reverse primers were ordered from Basilky and forward and reverse CERK primers were ordered from Macrogen. Detergent-compatible protein assay kit, 4%-20% SDS-PAGE gels, and 2X Laemmli sample buffer were purchased from Bio-Rad (Hercules, CA, USA). Nitrocellulose membranes were purchased from Bio-Rad (Hercules, CA, USA). C1P was purchased from Avanti Polar Lipids (Alabaster, AL, USA). GKT137831 was purchased from Cayman Chemical (Ann Arbor, Michigan, USA). FlexiTube SMPDL3b-specific siRNA (5 nmol), NOX1-specific siRNA (5 nmol), and Hi-Perfect transfection reagent were purchased from Qiagen (Hilden, Germany). NBD-C1P was purchased by Echelon Biosciences Inc. (Salt Lake City, UT, USA).

2.2 | GEnc cell culture, irradiation and treatment

Human glomerular endothelial were cultured and differentiated in EGM-2 containing 2% of FBS and 1% of penicillin/streptomycin as previously described.[12] Briefly, conditionally immortalized endothelial cells were propagated at 33 degrees, and then, thermoshifted for differentiation for 5 days at 37 degrees. A single dose of 4Gy was delivered from an RS2000 X-ray irradiator (225 kV) according to the manufacturer's specifications (Rad Source Technologies, Suwanee, GA, USA). The dose rate was adjusted to 265 cGy/min. For C1P treatment, cells were cultured in 96-well plates and pretreated for 24 hours with 30 μM of C1P. Prior to treatment, the C1P double-distilled water solution was sonicated at

4 degrees to ensure proper dispersion. Cells were then irradiated (4Gy) and treatment was stopped by removing the media and adding cold saline solution at the proper time points. For GKT treatment, cells were directly irradiated after treatment with 20 μM of GKT dissolved in DMSO. An equal quantity of DMSO was added to the control samples.

2.3 | Transfection with SMPDL3b-specific or NOX1-specific siRNA

For transfection, GEnC were cultured in 6-well plates (for western blot) or 24 mm dishes (for imaging purposes) and transfected with SMPDL3b-specific siRNA or NOX1-specific siRNA, respectively. Control siRNA was also used as per the manufacturer's protocol. Hi-Perfect transfection reagent was added, and the cells were incubated with the siRNA mixture for 24 hours after complete differentiation. Cells were then radiated, incubated again for 24 hours, and either scraped for western blot or stained with DHE for imaging.

2.4 | Immunofluorescence with DHE and DAPI

For quantification of mean immunofluorescence (MIF), cells were stained with DHE for 30 minutes at 37°C, fixed and stained with DAPI, then visualized using Zeiss confocal microscope (LSM710 Meta, Carl Zeiss, Inc, Thornwood, NY, USA). Data were analyzed using the LSM Image Browser Software.

2.5 | Quantitative RT-PCR

Cells were washed with ice-cold PBS and RNA extraction was carried out according to the manufacturer's protocol of the RNA minieasy kit (Qiagen, Hilden, Germany). RNA was quantified by NanoDrop (Thermo Fischer Scientific) and converted to cDNA using a SuperScript III First-Strand Synthesis kit (Thermo Fischer Scientific). The cDNA was then diluted (1:25) and 2 μL were added per 25 μL of reaction. Using the Perfecta SYBR Green FastMix (Quantabio), the reaction was executed in real-time PCR system (Applied Biosystems, Foster City, CA, USA) as previously described.[17] Real-time quantitative PCR was done for Nox1, Nox4, and glyceraldehyde-3-phosphate dehydrogenase (GAPDH). The following primer sequences were used: 5′-gTCAgTggTggACCTgAC CT-3′ (H-GAPDH F); 5’-gTCAACggTACATCTggggA-3′ (H-GAPDH R); 5′-gACAgCAgATTgCgACACACA-3′ (H-NOX1 R); 5′-CACAAgAAAAATCCTTgggTCAA-3′ (H-NOX1 F); 5′-CAATCCgTgTgggTgAA-3′ (H-CERK F); 5′-TTggTcTggACgTCAgCTTC-3′ (H-CERK R).

2.6 | Protein extraction and western blotting

Endothelial cells were homogenized in cold RIPA buffer supplemented with 20 μL of protease and phosphatase inhibitor cocktail. Protein quantification was done using Lowry Reagent assay kit from Sigma-Aldrich. Samples were then prepared after quantification with 2X Laemmli sample buffer (Bio-Rad). An equal amount of proteins (25–30 μg) were then loaded into 12.5% of SDS-PAGE gels (Bio-Rad) and transferred on nitrocellulose membrane overnight at 300 mA. The membranes were then blocked with 5% of skimmed milk or BSA in Tris-saline solution for 1 hour at room temperature. The following primary antibodies were used, each according to the protocol suggested by the manufacturer: rabbit polyclonal anti-SMPDL3b (1:1000) (Genway Biotech, Inc, San Diego, CA, USA), mouse-monoclonal

anti-GAPDH (1:1000) (Abcam), rabbit monoclonal NOX1 and NOX4 antibodies (1:250) (Abcam), mouse polyclonal caspase 9 antibody (1:1000) (Cell Signaling), rabbit polyclonal CERK antibody (1:500). The membranes were incubated with the primary antibodies overnight then washed three times for 10 minutes each in Tris-saline solution with 0.1% of Tween 20. HRP conjugated secondary antibodies were used and the images were developed using enhanced chemiluminescence (Bio-Rad). Densitometry was performed using the ImageJ software (National Institute of Health, Bethesda, MD, USA).

2.7 | NOX assay

The activity of the NADPH enzymes was assessed in cultured GEnC as previously described.[20,21] Cultured endothelial cells were washed three times with ice-cold PBS and scraped from the plate. They were then centrifuged at 800 *g* for 10 minutes at 4 degrees. Pellets were obtained and the supernatant was discarded. The pellet was suspended with a special lysis buffer (20 mM KH_2PO_4 [pH 7.0], 1 mM EGTA, 1 mM phenylmethylsulfonyl fluoride, 10 μg/mL aprotinin, and 0.5 μg/mL leupeptin). The homogenate was quantified using the Bio-Rad protein assay reagent. The assay was conducted on 50 μg of homogenates which were added to 50 mM of phosphate buffer (pH 7.0) containing 1 mM of EGTA, 150 mM of sucrose, 5 μM of lucigenin, and 100 μM of NADPH. Light emission was measured after 30 seconds for 8 minutes in a luminometer. The first and last readings were discarded, and a buffer blank was subtracted from each reading. Superoxide production was averaged and expressed as relative light units/min.mg of protein.

2.8 | Phosphodiesterase enzymatic activity assay

C1P phosphatase assay was conducted as described by Mitrofanova et al.[18] About 50 μM of C6-NBD-C1P complexed to 10 μM of BSA was incubated with homogenates (8 μg of protein) in 200 mM of NaCl, 2 mM of EDTA, 100 mM of HEPES, pH 7.4, and a protease inhibitor cocktail (1:200) for 10 minutes at 37°C. The reaction was then terminated by 3.75 volumes of chloroform:methanol (1:2), 1.25 volume of 100% chloroform and 1.25 volumes of 2 M KCl/0.2 M H3PO4. The lower phase was dried using speed vacuum and subsequently resolved by thin layer chromatography (TLC) on Silica Gel plates using chloroform:methanol: acetic acid: 15 mM of CaCl2 (60:35:2:4, v/v/v/v) as developing solvent.

2.9 | Liquid chromatography-mass spectrometry analysis

Cell pellets containing 10^6 cells per sample were subjected to liquid extraction. Liquid chromatography-mass spectrometry (LC-MS) analysis of sphingolipids was performed at the lipidomic core facility at the Medical University of South Carolina using electrospray ionization/tandem mass spectrometry on a mass spectrometer (Quantum; Thermo Fischer Scientific) as previously described.[22]

2.10 | Animal studies

To assess endothelial cell damage in vivo, 10 weeks old C57BL6 male mice were treated with normal saline (NS), GKT, or C1P with or without a single dose of 14 Gy. GKT treatment was administered at 40 mg/kg/day by oral gavage, whereas the other groups

received either a daily intraperitoneal injection of 30 mg/kg C1P C16:0 or 0.9% of NS for 28 days. To prepare a stock solution (5mg/ml), C1P C16:0 powder was weighed and dissolved in 0.9% of NS and 2.5% of DMSO by sonication. Aliquots were stored at −20°C, then melted, and sonicated once again before application.

Mice were irradiated using an image guided small animal arc radiation treatment system (iSMAART). iSMAART was developed to achieve highly precise radiation targeting through the utilization of onboard cone beam computed tomography (CBCT) guidance.[23] Mice were anesthetized with ketamine/xylazine. Both kidneys were harvested and processed for histological-immunohistochemical studies.

2.11 | Immunofluorescence staining

To study endothelial cell damage, slides with tissue sections (5 μ) were deparaffinized and exposed to heat-induced antigen retrieval using Biocare de-cloaking chamber in pH 6 citrate buffer (Target Retrieval Solution, Citrate pH 6, Dako, USA), followed by peroxidase (Peroxidase-1, Biocare Medical, USA) and protein block (Background Sniper, Biocare-Medical, USA) for 10 mins each. Blocking and antibody staining were performed with Biocare autostainer, Nemesis 3600 (Biocare Medical, USA). TUNEL staining was performed with TUNEL Assay Kit - BrdU-Red (ab66110) as per the manufacturer's instructions. Mouse monoclonal affinity-purified primary antibody for CD31 (Abcam, USA) was applied at 4°C overnight and the secondary antibody goat anti-mouse (Abcam, USA) was used for 1 hour. The slides were dehydrated and sealed with a coverslip and sealant. Images were acquired using a Zeiss confocal microscope (LSM700 META; Carl Zeiss, Inc) via a 63× oil objective lens in different planes using a Z-series pattern with a step size of 0.5 μm. During analysis, individual planes were deconvoluted and stacked to produce a maximum projected image and minimize the overlap of cells. A minimum of 30 images was captured per group. Image processing for scale bar was performed by *Fiji software*. Fluorescence intensity was measured using ImageJ software. CD31 cells positive for TUNEL were counted manually for around 30 glomeruli per group.

2.12 | Statistical analysis

Results were expressed as the means ± SE. One-way ANOVA was used to compare groups and results were considered statistically significant if $P < .05$ (Graph Pad Prism software; La jolla, CA, USA).

3 | RESULTS

In order to study radiation-induced damage to GEnC, we established a logarithmic dose-response curve using the clonogenic assay on non-differentiated cells (Figure 1). The percentage of cell survival, measured by the ability of the cells to form detectable colony units, decreased by 50% at 2 Gy compared to the control, nonirradiated condition. No colonies were detected at a dose of 8 Gy indicating a lack of cell viability.

Recent work from our group has implicated sphingolipids in mediating cellular responses to stressors such as radiation.[6,24] Therefore, we investigated whether the observed changes in cell viability are associated with changes in the sphingolipid profile of GEnC. To that

end, differentiated cells were irradiated at a single dose of 4 Gy, lipids were extracted at different time points of 30 minutes, 6, 12, 18, and 24 hours and were analyzed by mass spectrometry. The analysis revealed a gradual temporal increase in total ceramide levels post-irradiation (Figure 2A). This change was mainly due to a significant increase in long and very long-chain ceramide species, namely those with C16 and C24:1 acyl chains (Figure 2B). In parallel with the changes in ceramide levels, there was a gradual and significant drop in the total levels of C1P, with the greatest decrease observed at 24 hours post-irradiation (Figure 2C).

Next, we investigated the mechanism of C1P downregulation post-radiation. To this end, we conducted western blot and real-time PCR on radiated GEnC. The mRNA and protein levels of ceramide kinase (CERK) revealed no significant changes at 24 hours post-irradiation (Figure 2D). Given our knowledge of the role of SMPDL3b as a lipid modifying enzyme and its implication in radiation-induced podocytopathy,[6] we investigated changes in the levels of SMPDL3b in the response of GEnC to radiation. Western blotting analysis revealed a gradual and time-dependent increase in the protein levels of SMPLD3b starting at 12 hours post-irradiation, with the increase going beyond 2-fold at 24 hours (Figure 2E). Recent work suggested a role for SMPDL3b in C1P dephosphorylation,[18] which prompted us to conduct a phosphatase assay. Our results show a significant elevation in phosphatase activity at 12 and 24 hours post-IR (Figure 2F). Taken together, these results suggest a role for SMPDL3b in C1P modulation post-radiation exposure.

It has been well established that oxidative stress is involved is IR-induced tissue injury.[25,26] To that end, we investigated the production of ROS in GEnC post-irradiation. Cells were irradiated and stained with DHE and DAPI. The results showed an incremental and temporal increase in oxidative stress with significant ROS production at 2 and 24 hours after treatment (Figure 3A,B).

To further investigate the observed oxidative response, we conducted the NOX assay on differentiated endothelial cells after radiation exposure at different time points. Experimental results revealed a time-dependent increase in the enzymatic activity of NOXs post-irradiation. In addition, administration of exogenous C1P (30 μM) decreased the the activity of NOX enzymes significantly both at 2 and 24 hours post-irradiation (Figure 3C). This hints that there might be a feedback mechanism at play between the levels of C1P and NOX activity.

A variety of NOXs have been identified and discussed in the literature, ranging from NOX1 to NOX5, in addition to DUOX1 & 2.[27] For our purpose, NOX1 & 4 are the major isoforms expressed in human endothelial cells.[28–30] Therefore, we investigated the change in the protein levels of these two NOXs in response to radiation injury. Only NOX1 showed a significant and time-dependent increase, peaking at 24 hours post-irradiation (Figure 3D), whereas NOX4 level showed no significant changes (Figure 3E). In parallel, NOX1 gene expression revealed an incremental trend with a significant peak 2 hours after irradiation (Figure 3F). To further verify the role of NOX1 in our model, oxidative stress (OS) was assessed using DHE after silencing NOX1 using NOX1-specific siRNA (Figure 3G). Indeed, knockdown of NOX1 was able to significanly reduce superoxide anion generation

post-irradiation (Figure 3H). Therefore, NOX1 is the major culprit in IR-induced oxidative stress in GEnC.

We next wanted to research the role of SMPDL3b, NOXs, and the changes in the spingolipidomic profile in the viability of endothelial cells post-IR. For this purpose, GEnC were irradiated and survival was assayed in the presence or absence of GKT or C1P administration. In non-treated endothelial cells, survival dropped significantly to around 35% after irradiation. However, treatment with GKT (20 μM) or C1P (30 μM) partially restored cell survival (Figure 4A). This suggests that the increase in NOX levels and activity and the drop in C1P levels are key mediators of IR-induced injury in GEnC.

We then aimed to establish the role of SMPDL3b in radiation-induced endothelial cell damage. Hence, we proceeded with silencing SMPDL3b expression in cultured GEnC using siRNA technology. We were able to achieve a 75% reduction in the protein expression levels of SMPDL3b (Figure 4B). Of note, silencing of SMPDL3b using siRNA did not yield any significant effect neither on CERK mRNA nor its protein level (Figure 4C). We then assessed the effect of SMPDL3b knockdown on radiation response of GEnC. Indeed, knockout of SMPDL3b decreased caspase-3 cleavage and improved the survival of radiated glomerular endothelial cells (Figure 4D). However, the levels of radiation-iduced caspase 9 cleavage did not significantly change upon silencing SMPDL3b (Figure 4E). These results implicate SMPDL3b in radiation-induced GEnC injury in a caspase-dependent pathway.

We then investigated the interplay between SMPDL3b and oxidative stress since both are implicated in GEnC response due to radiation. To that end, we studied the change in the levels of expression of SMPDL3b in radiated cells treated with GKT. Expression levels of SMPDL3b increased 24 hours post-radiation. However, pretreatment with GKT restored the levels of SMPDL3b post-radiation almost back to baseline levels (Figure 4F). This suggests that ROS production by NOXs is upstream of SMPDL3b during radiation stress.

Next, we proceeded to verify the results obtained in our cell line using an in vivo model. To that end, C57BL6 male mice were treated with NS, GKT, or C1P prior to focal renal radiation (14 Gy). After 24 hours, the survival of endothelial cells was checked via TUNEL assay on kidney sections. The platelet endothelial cell adhesion molecule (PECAM-1), also known as cluster of differentiation 31 (CD31), was used as a marker for endothelial cells. Percentage of CD31 positive cells with TUNEL positivity was quantitated. The results indicate a significant increase in endothelial cell apoptosis post-radiation. Murine endothelial cells could be partially rescued from damage when mice are treated with GKT or C1P (Figure 5A,B). Treatment in each of the latter cases restored cell survival almost back to basal levels post-radiation. These results strongly implicate oxidative stress and C1P in radiation-induced glomerular endothelial cell injury.

4 | DISCUSSION

Our results implicate a novel pathway in radiation-induced injury of glomerular endothelial cells. Analysis of radiated GEnC reveals that endothelial cell damage is associated with a disruption in the intracellular lipid homeostasis with an associated increase in the lipid-

modifying enzyme SMPDL3b, an increase in long-chain ceramide species and a decrease in the level of their phosphorylated metabolites. Treatment with C1P in an attempt to restore normal lipid levels partially attenuates cell death. Further analysis implicates NOX1 and NOX-derived ROS in the endothelial cell damage as well as in the observed lipid changes. Treatment with GKT (a dual NOX inhibitor) partially restores cell survival and decreases the levels of SMPDL3b. In addition, knockdown of SMPDL3b decreases radiation-mediated cellular injury.

Our work using GEnC extends prior knowledge on ceramide and its bioactive metabolites. C1P is a potent sphingolipid which has been implicated in the regulation of both cell growth and survival in a wide array of cell types.[31–35] The mitogenic and pro-survival effects of C1P have been extensively investigated[36] and involve a set of downstream cell transduction processes such as ERK1 and 2/ c-JNK and the mTOR/p70S6K pathways.[32,37] Since our cell line is terminally differentiated, the mechanism of action of C1P is more likely to be pro-survival than mitogenic; however, the signaling pathways involved are yet to be established. In contrast to C1P, it is thought that the major role of ceramide in cell signaling is to promote cell cycle arrest and subsequently lead to cell death through pathways which have been extensively discussed in the literature.[38] The changes reported in the sphingolipidomic profile of GEnC upon delivery of radiation are novel. The drop in the concentration of different species of C1P and the significant increase in the levels of ceramide can be tightly correlated to the results of the clonogenic assay, which showed a concomitant decrease in the survival rate of the irradiated cells. Exogenous treatment of the cultured GEnC with C1P decreased the sensitivity of the cells to radiation and lead to partial restoration of survival, further implicating the role of C1P depletion in radiation-induced endothelial cell injury. This suggests that radiation causes injury to the GEnC through tilting the balance between the C1P and ceramide species.

In contrast to podocytes, which downregulate SMPDL3b after exposure to radiation,[6] GEnC upregulate the level of SMPDL3b. Hence, the lipid-modifying enzyme SMPDL3b has a differential response to radiation that is cell-type specific. In GEnC, SMPDL3b signals radiation response through altering the C1P/ceramide balance resulting in downtream activation of caspase 3. Recent work established SMPDL3b as a C1P-interacting protein which can also bind to CERK.[13] In addition, overexpression of SMPDL3b was reported to increase the conversion of C1P into ceramide.[18] These results are corroborated by our finding that radiation increases levels of SMPDL3b and phosphatase activity along with drop in C1P levels.

Irradiation is genotoxic with direct and indirect effects on cellular DNA.[39] Genomic stress is associated with increased generation of ROS and the majority of studies implicate NOX in ROS-mediated cellular damage.[40] Exposure of several cell types to radiation was shown to induce NOX upregulation and subsequent generation of superoxides and hydrogen peroxide.[41,42] For example, the acute exposure of keratinocytes to both types of UV radiation, UVA and UVB, resulted in increased production of NOX-generated ROS.[43–45] Several studies have implicated this pathway in radiation-induced cell death.[40,42,46] In fact, NOXs are culprits in a wide array of pathologies, especially those related to the renal system. Studies conducted by Eid et al have elucidated the various biochemical

consequences of NOX activation in diabetic kidney disease and the role of NOX-induced oxidative stress in kidney epithelial cell damage and podocytopathy.[20,21,47] In addition, research on vascular endothelial cells has shown that inflammatory cytokines such as TNF-α and atherogenic remnant deposition can induce apoptosis of these cells through NOX-dependent pathways.[48] Our findings extend this body of literature to implicate NOX in radiation-induced injury of GEnC.

Our results demonstrate that exposure of cultured GEnC to IR leads to an increase in the levels of NOX1, and subsequent cell death downstream of the NOX-ROS pathway. Inhibition of this pathway by GKT, reverses the observed injury and partially restores cell survival. In vivo, treatment of mice with GKT reduced glomerular endothelial cell apoptosis post-radiation. Hence, targeting oxidative stress and NOX enzymes could prove to be radioprotective.

We then proceeded to investigate whether the observed lipidomic changes and the NOX-ROS pathways are related at a molecular level. Indeed, treatment with GKT leading to inhibition of NOX enzymes reduced not only cell death, but also restored basal levels of expression of SMPDL3b. This suggests that SMPDL3b is downstream of NOX1 in GEnC damage upon exposure to radiation.

To our knowledge, this is the first time a link is established between the NOX pathway, SMPDL3b, and sphingolipids in radiation-induced damage. This reveals an exciting insight into the interplay between major signal transduction pathways that mediate many of the known physiological and pathophysiological functions of endothelial cells. Given the importance of the glomerular endothelial cell in maintaining proper kidney filtration, our data can be of promising clinical significance. The proposed pathway poses SMPDL3b as a novel therapeutic target for renal radioprotection in cancer patients treated with RT (Figure 6).

ACKNOWLEDGMENTS

Y.Z is funded by MPP grant from the American Univerity of Beirut. BM. AF is funded by US National Institutes of Health Grants DK104753 and DK090316. BM is funded by R01 CA227493.

Funding information

National Institutes of Health (NIH), Grant/Award Number: 1R01CA227493–01; AUB MPP Award, Grant/Award Number: 320166

Abbreviations:

GEnC	human glomerular endothelial cells
IR	ionizing radiation
SMPDL3b	sphingomyelin phosphodiesterase acid-like 3B
NOX	NADPH oxidase
ROS	reactive oxygen species

REFERENCES

1. Cassady JR. Clinical radiation nephropathy. Int J Radiat Oncol Biol Phys. 1995;31(5):1249–1256. [PubMed: 7713786]
2. Dawson LA, Kavanagh BD, Pauliono AC, et al. Radiation-associated kidney injury. Int J Radiat Oncol Biol Phys. 2010;76(Suppl. 3):S108–S115. [PubMed: 20171504]
3. Cohen EP, Robbins ME. Radiation nephropathy. Semin Nephrol. 2003;23(5):486–499. [PubMed: 13680538]
4. Luxton RW. Radiation nephritis. A long-term study of 54 patients. Lancet. 1961;2(7214):1221–1224. [PubMed: 14467525]
5. Yang GY, May KS, Iyer RV, et al. Renal atrophy secondary to chemoradiotherapy of abdominal malignancies. Int J Radiat Oncol Biol Phys. 2010;78(2):539–546. [PubMed: 20133075]
6. Ahmad A, Mitrofanova A, Bielawski J, et al. Sphingomyelinase-like phosphodiesterase 3b mediates radiation-induced damage of renal podocytes. FASEB J. 2017;31(2):771–780. [PubMed: 27836988]
7. Abou Daher A, El Jalkh T, Eid A, et al. Translational aspects of sphingolipid metabolism in renal disorders. Int J Mol Sci. 2017;18(12):2528. [PubMed: 29186855]
8. Zeidan YH, Hannun YA. Translational aspects of sphingolipid metabolism. Trends Mol Med. 2007;13(8):327–336. [PubMed: 17588815]
9. Merscher S, Fornoni A. Podocyte pathology and nephropa-thy—sphingolipids in glomerular diseases. Front Endocrinol (Lausanne). 2014;5(127):1–11. [PubMed: 24474947]
10. Stewart FA. Radiation nephropathy after abdominal irradiation or total-body irradiation. Radiat Res. 1995;143(3):235–237. [PubMed: 7652159]
11. Kim JH, Jenrow KA, Brown SL. Mechanisms of radiation-induced normal tissue toxicity and implications for future clinical trials. Radiat Oncol J. 2014;32(3):103–115. [PubMed: 25324981]
12. Satchell SC, Tasman CH, Singh A, et al. Conditionally immortalized human glomerular endothelial cells expressing fenestrations in response to VEGF. Kidney Int. 2006;69(9):1633–1640. [PubMed: 16557232]
13. Mallela SK, Mitrofanova A, Merscher S, et al. Regulation of the amount of ceramide-1-phosphate synthesized in differentiated human podocytes. Biochim Biophys Acta Mol Cell Biol Lipids. 2019;1864(12):158517. [PubMed: 31487557]
14. Mitrofanova A, Sosa MA, Fornoni A. Lipid mediators of insulin signaling in diabetic kidney disease. Am J Physiol Renal Physiol. 2019;317(5):F1241–F1252. [PubMed: 31545927]
15. Pullen N, Fornoni A. Drug discovery in focal and segmental glomerulosclerosis. Kidney Int. 2016;89(6):1211–1220. [PubMed: 27165834]
16. Wahl P, Ducasa GM, Fornoni A. Systemic and renal lipids in kidney disease development and progression. Am J Physiol Renal Physiol. 2016;310(6):F433–F445. [PubMed: 26697982]
17. Fornoni A, Sageshima J, Wei C, et al. Rituximab targets podocytes in recurrent focal segmental glomerulosclerosis. Sci Transl Med. 2011;3(85):85ra46.
18. Mitrofanova A, Mallela SK, Ducasa GM, et al. SMPDL3b modulates insulin receptor signaling in diabetic kidney disease. Nat Commun. 2019;10(1):2692. [PubMed: 31217420]
19. Yoo T-H, Pedigo CE, Guzman J, et al. Sphingomyelinase-like phosphodiesterase 3b expression levels determine podocyte injury phenotypes in glomerular disease. J Am Soc Nephrol. 2015;26(1):133–147. [PubMed: 24925721]
20. Eid AA, Ford BM, Block K, et al. AMP-activated protein kinase (AMPK) negatively regulates Nox4-dependent activation of p53 and epithelial cell apoptosis in diabetes. J Biol Chem. 2010;285(48):37503–37512. [PubMed: 20861022]
21. Eid AA, Gorin Y, Fagg BM, et al. Mechanisms of podocyte injury in diabetes: role of cytochrome P450 and NADPH oxidases. Diabetes. 2009;58(5):1201–1211. [PubMed: 19208908]
22. Bielawski J, Szulc ZM, Hannun YA, et al. Simultaneous quantitative analysis of bioactive sphingolipids by high-performance liquid chromatography-tandem mass spectrometry. Methods. 2006;39(2):82–91. [PubMed: 16828308]
23. Sha H, Udayakumar TS, Johnson PB, et al. An image guided small animal stereotactic radiotherapy system. Oncotarget. 2016;7(14):18825–18836. [PubMed: 26958942]

24. Zeidan YH, Jenkins RW, Hannun YA. Remodeling of cellular cytoskeleton by the acid sphingomyelinase/ceramide pathway. J Cell Biol. 2008;181(2):335–350. [PubMed: 18426979]
25. Robbins ME, Zhao W. Chronic oxidative stress and radiation-induced late normal tissue injury: a review. Int J Radiat Biol. 2004;80(4):251–259. [PubMed: 15204702]
26. Riley PA. Free radicals in biology: oxidative stress and the effects of ionizing radiation. Int J Radiat Biol. 1994;65(1):27–33. [PubMed: 7905906]
27. Bedard K, Krause KH. The NOX family of ROS-generating NADPH oxidases: physiology and pathophysiology. Physiol Rev. 2007;87(1):245–313. [PubMed: 17237347]
28. Ago T, Kitazono T, Kuroda J, et al. NAD(P)H oxidases in rat basilar arterial endothelial cells. Stroke. 2005;36(5):1040–1046. [PubMed: 15845888]
29. Hu T, et al. Reactive oxygen species production via NADPH oxidase mediates TGF-beta-induced cytoskeletal alterations in endothelial cells. Am J Physiol Renal Physiol. 2005;289(4):F816–F825. [PubMed: 16159901]
30. Kobayashi S, Nojima Y, Shibuya M, et al. Nox1 regulates apoptosis and potentially stimulates branching morphogenesis in sinusoidal endothelial cells. Exp Cell Res. 2004;300(2):455–462. [PubMed: 15475009]
31. Presa N, Gomez-Larrauri A, Dominguez-Herrera A, et al. Novel signaling aspects of ceramide 1-phosphate. Biochim Biophys Acta Mol Cell Biol Lipids. 2020;1865(4):158630. [PubMed: 31958571]
32. Gangoiti P, Granado MH, Wang SW, et al. Ceramide 1-phos-phate stimulates macrophage proliferation through activation of the PI3-kinase/PKB, JNK and ERK1/2 pathways. Cell Signal. 2008;20(4):726–736. [PubMed: 18234473]
33. Miranda GE, Abrahan CE, Agnolazza DL, et al. Ceramide-1-phosphate, a new mediator of development and survival in retina photoreceptors. Invest Ophthalmol Vis Sci. 2011;52(9):6580–6588. [PubMed: 21724910]
34. Gangoiti P, Bernacchioni C, Donati C, et al. Ceramide 1-phos-phate stimulates proliferation of C2C12 myoblasts. Biochimie. 2012;94(3):597–607. [PubMed: 21945811]
35. Mitra P, Maceyka M, Payne SG, et al. Ceramide kinase regulates growth and survival of A549 human lung adenocarcinoma cells. FEBS Lett. 2007;581(4):735–740. [PubMed: 17274985]
36. Gomez-Munoz A, Gangoiti P, Granado MH, et al. Ceramide-1-phosphate in cell survival and inflammatory signaling. Adv Exp Med Biol. 2010;688:118–130. [PubMed: 20919650]
37. Gangoiti P, Arana L, Ouro A, et al. Activation of mTOR and RhoA is a major mechanism by which ceramide 1-phosphate stimulates macrophage proliferation. Cell Signal. 2011;23(1):27–34. [PubMed: 20727406]
38. Gómez-Muñoz A Ceramide 1-phosphate/ceramide, a switch between life and death. BBA Biomembranes. 2006;1758(12): 2049–2056. [PubMed: 16808893]
39. Yang J, Yu Y, Hamrick HE, Duerksen-Hughes PJ. ATM, ATR and DNA-PK: initiators of the cellular genotoxic stress responses. Carcinogenesis. 2003;24(10):1571–1580. [PubMed: 12919958]
40. Coates PJ, Lorimore SA, Wright EG. Cell and tissue responses to genotoxic stress. J Pathol. 2005;205(2):221–235. [PubMed: 15643669]
41. Collins-Underwood JR, Zhao W, Sharpe JG, et al. NADPH oxidase mediates radiation-induced oxidative stress in rat brain microvascular endothelial cells. Free Radic Biol Med. 2008;45(6):929–938. [PubMed: 18640264]
42. Tateishi Y, Sasabe E, Ueta E, et al. Ionizing irradiation induces apoptotic damage of salivary gland acinar cells via NADPH oxidase 1-dependent superoxide generation. Biochem Biophys Res Commun. 2008;366(2):301–307. [PubMed: 18035043]
43. Wang H, Kochevar IE. Involvement of UVB-induced reactive oxygen species in TGF-beta biosynthesis and activation in keratinocytes. Free Radic Biol Med. 2005;38(7):890–897. [PubMed: 15749385]
44. Van Laethem AN, Nys K, Van Kelst S, et al. Apoptosis signal regulating kinase-1 connects reactive oxygen species to p38 MAPK-induced mitochondrial apoptosis in UVB-irradiated human keratinocytes. Free Radic Biol Med. 2006;41(9):1361–1371. [PubMed: 17023263]

45. Valencia A, Kochevar IE. Nox1-based NADPH oxidase is the major source of UVA-induced reactive oxygen species in human keratinocytes. J Invest Dermatol. 2008;128(1):214–222. [PubMed: 17611574]

46. Azzam EI, et al. Oxidative metabolism modulates signal transduction and micronucleus formation in bystander cells from alpha-particle-irradiated normal human fibroblast cultures. Cancer Res. 2002;62(19):5436–5442. [PubMed: 12359750]

47. Eid S, Boutary S, Braych K, et al. mTORC2 signaling regulates Nox4-induced podocyte depletion in diabetes. Antioxid Redox Signal. 2016;25(13):703–719. [PubMed: 27393154]

48. Shin HK, Kim YK, Kim KY, et al. Remnant lipoprotein particles induce apoptosis in endothelial cells by NAD(P)H oxidase-mediated production of superoxide and cytokines via lectin-like oxidized low-density lipoprotein receptor-1 activation: prevention by cilostazol. Circulation. 2004;109(8):1022–1028. [PubMed: 14967724]

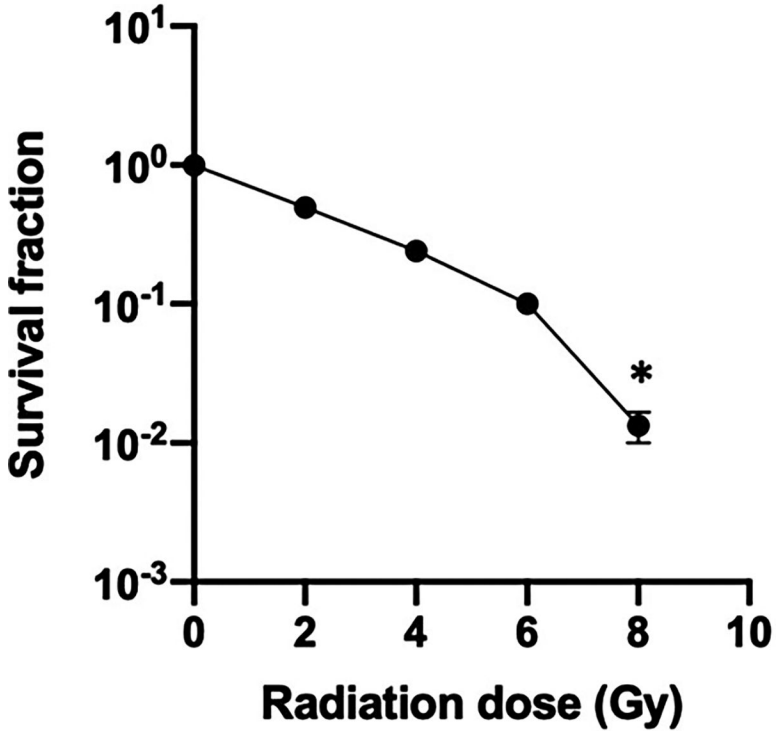

FIGURE 1.

Human glomerular endothelial cell logarithmic survival curve. Cultured endothelial cells were subjected to increasing doses of radiation, incubated at 37 degrees and the colony forming units (CFU) were counted under the microscope after staining with crystal violet. CFU were reported as percentage of control (nonirradiated cells). The results are representative of at least five independent experiments. *$P < .05$

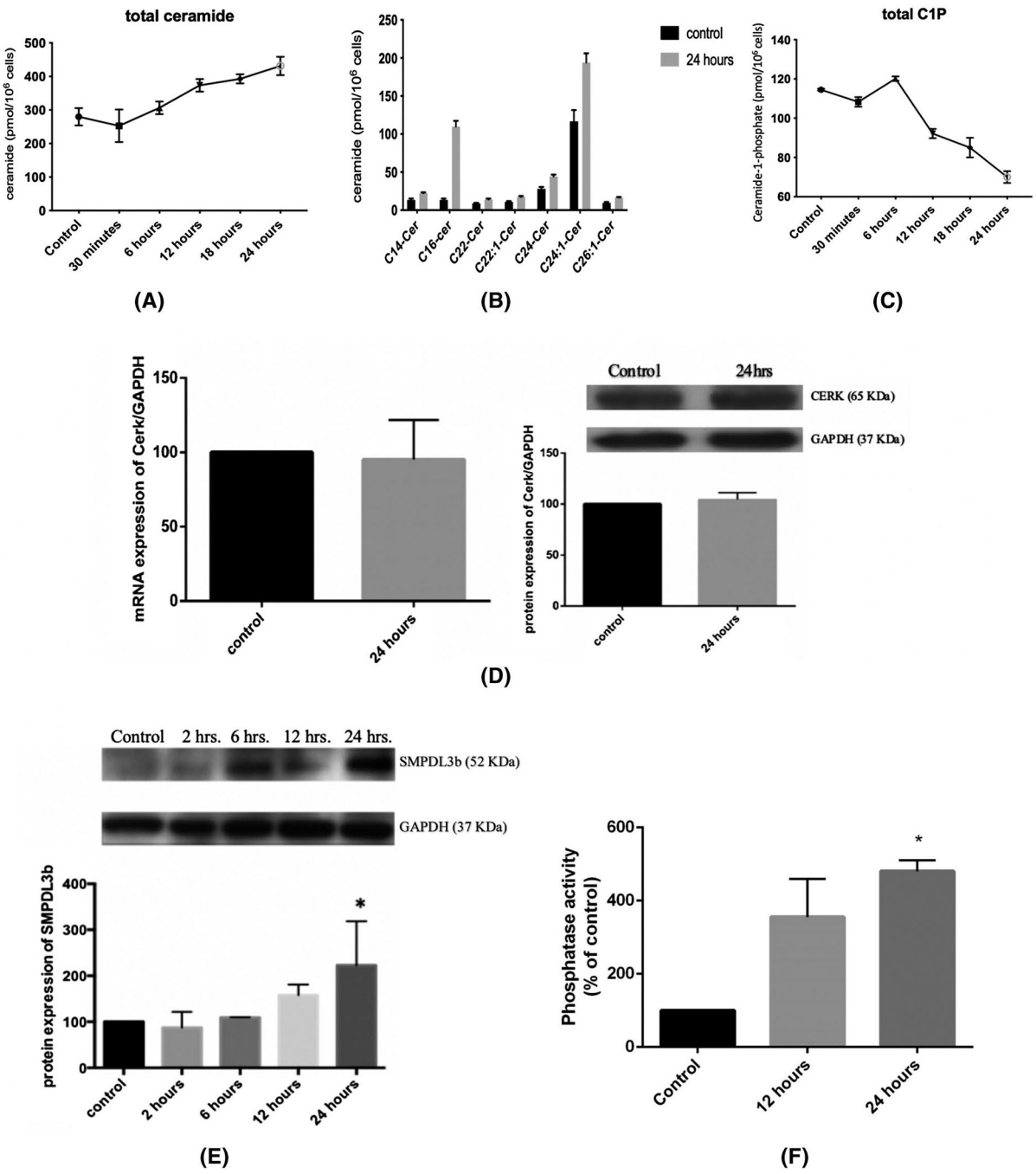

FIGURE 2.

Radiation leads to a significant alteration of the sphingolipid profile in GEnC. Cells were irradiated with 0 Gy (control) or 4 Gy, and pellets containing 10^6 cells were collected after 30 minutes, 6, 12, 18, and 24 hours. After extraction of lipids, the treatment groups were subjected to liquid chromatography-mass spectrometric analysis to determine the levels of total ceramide (A), the different ceramide sub-species (B), and the total level of C1P (C). Results represent the average of three independent experiments. D, Changes in the mRNA and protein levels of CERK at 24 hours post-irradiation. E, Changes in the level of

protein expression of SMPDL3b post-irradiation. All blots were quantified by densitometry using Image J software, normalized to the house-keeping gene GAPDH and expressed as percentage of control. F, C1P Phosphatase in vitro assay after radiation at 4 Gy using NBD-labeled C1P at 12- and 24-hours post-irradiation. Results shown are the mean values of at least four independent experiments. *$P < .05$

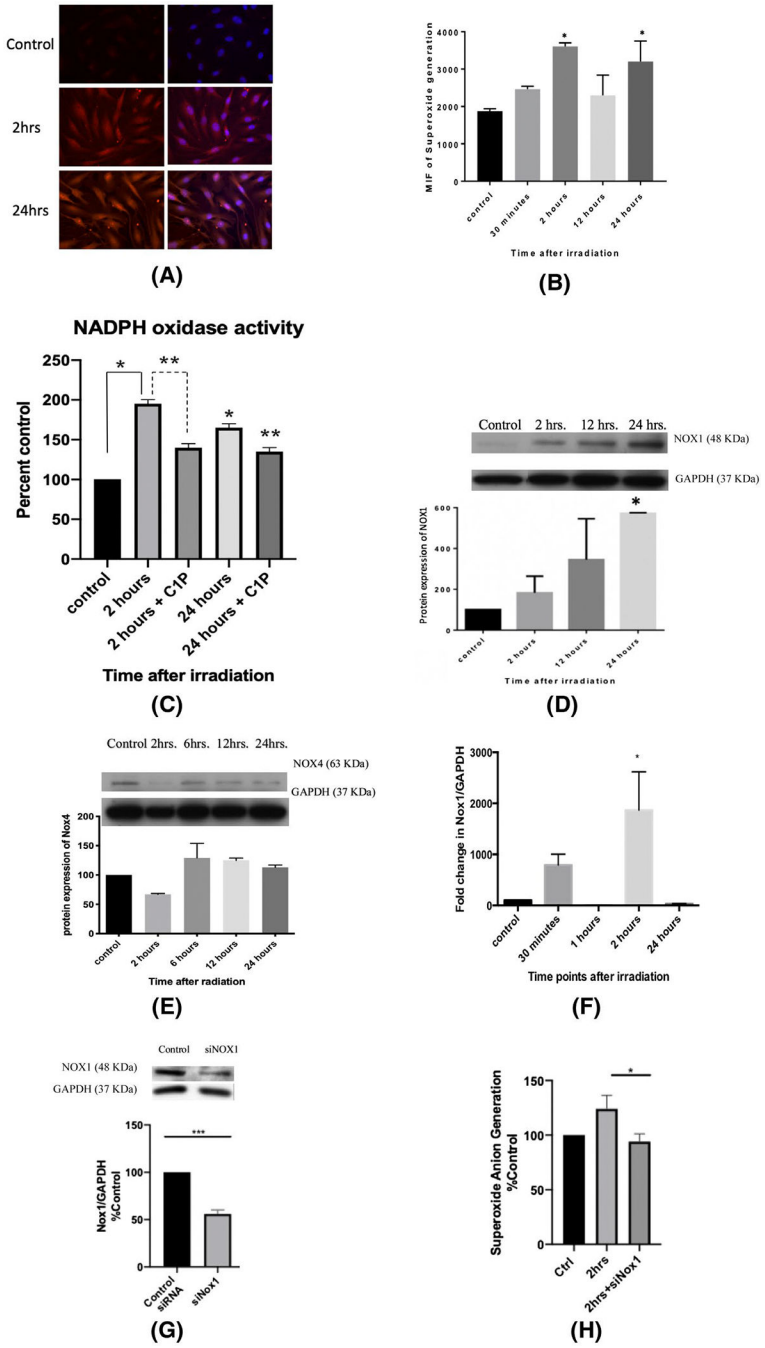

FIGURE 3.

Radiation increases superoxide anion generation by increasing the transcription and translation of NOX1. A, Immunofluorescence staining with DHE and DAPI of endothelial cells radiation at 0 Gy (control) and at 4 Gy, 2 and 24 hours post-irradiation. B, Quantification of mean immunofluorescence at baseline (control) and at 30 minutes, 2, 24, and 24 hours post-irradiation at 4 Gy. Cells were plated in T-25 flasks until 80% confluency, differentiated and then irradiated at 4 Gy. The pellets were collected at various time points. C, NADPH oxidase activity was assessed via a lucigenin-based assay with and

without C1P administration. Photon emission was quantified as percentage of control (0 Gy) after subtracting blank. D, NOX1 and (E) NOX4 protein levels post-IR were assessed using western blot. F, NOX1 gene expression profile at 30 minutes, 1, 2, and 24 hours post-irradiation. G, siRNA was used to knockdown NOX1 and the protein expression levels of NOX1 levels were analyzed after 24 hours of incubation. H, NOX1-knockout GEnC show a significant decrease in superoxide anion generation at 2 hours post-irradiation. Results shown are the mean values of three independent experiments. *$P < .05$ compared to control and **$P < .05$ compared to the treated condition in the NADPH oxidase assay

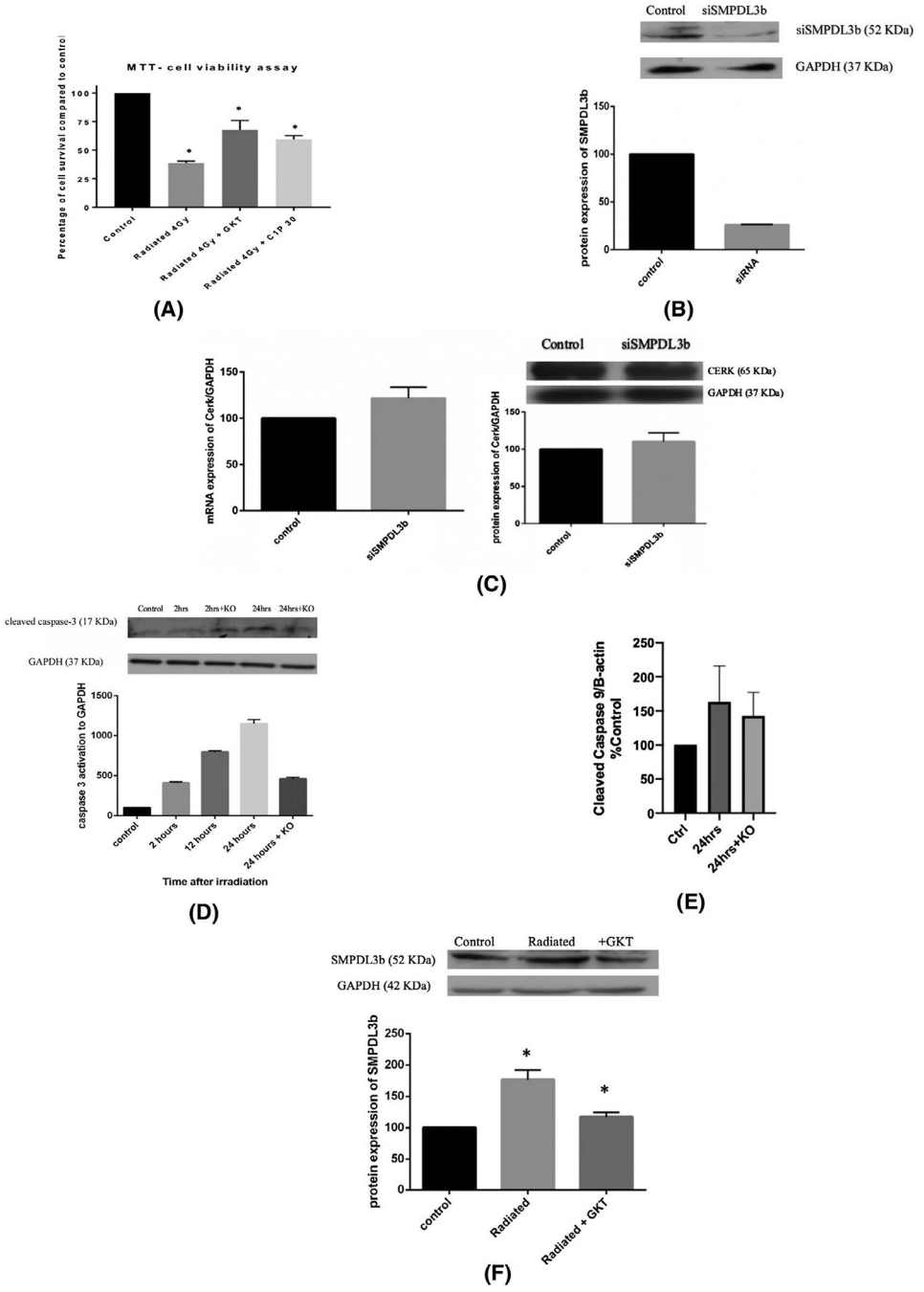

FIGURE 4.

SMPDL3b mediates IR-induced cell injury in a caspase-3 dependent mechanism. Endothelial cells were cultured in plates, differentiated, and treated either with siRNA, GKT, or C1P before irradiation at 4 Gy. A, Cell survival was assessed using MTT. Results were obtained by spectrophotometry. The readings were subtracted from blank and expressed as percentage relative to control. B, siRNA was used to knockdown SMPDL3b and the protein expression levels of SMPDL3b were analyzed after 24 hours of incubation. C, Changes in the mRNA and protein levels of CERK with siSMPDL3b. D, SMPDL3b-knockout GEnC

show improved survival post-irradiation as demonstrated by caspase-3 activation. Results are normalized to GAPDH and expressed as percentage to control. E, GEnC show no significant change in radiation-induced caspase-9 cleavage after SMPDL3b silencing (F) GKT treatment downregulates SMPDL3b protein expression post-radiation. Results were quantified by densitometry using Image J software, normalized to the house-keeping gene and expressed as percentage of control. Results are the mean of at least three independent experiments each done in triplicates. $*P < .05$

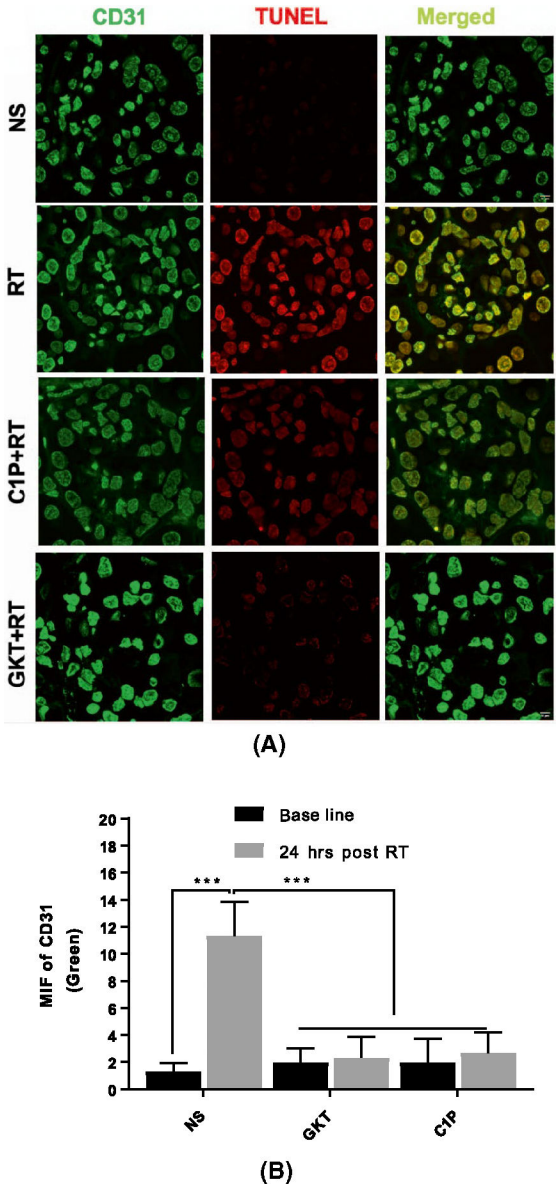

FIGURE 5.

Treatment with GKT or C1P improves glomerular endothelial cell viability in vivo. Murine kidneys were sectioned and processed for immunofluorescence co-staining of TUNEL with CD31. A, Images were captured using a Zeiss confocal microscope via a 63x oil objective lens in different planes using a Z-series pattern with a step size of 0.5 μm, scale bar 0.5 inches. B, Quantification of green fluorescence for CD31 and TUNEL (Red). Endothelial cell death increased significantly with IR. Treatment of mice with GKTor C1P restored cell survival to post-irradiation. Scale bar is 10 μm

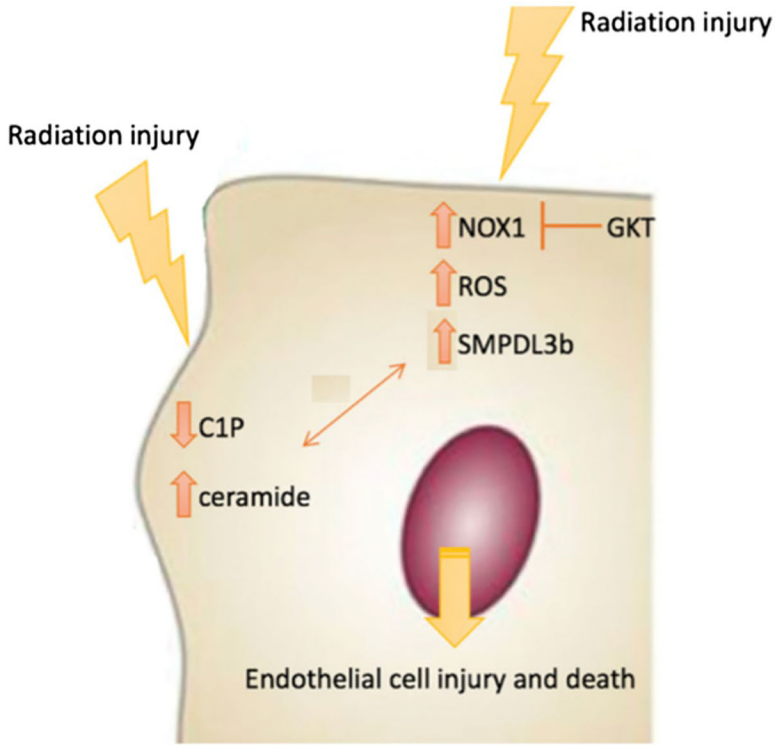

FIGURE 6.

Model of radiation-induced endothelial cell damage. The model depicts induction of NOX1 and NOX1-mediated reactive oxygen species (ROS) downstream radiation injury. The increase in SMPDL3b downstream of NOX1 is a key event in radiation injury of GEnC. This triggers changes in sphingolipid metabolism, including a drop in C1P and an increase in ceramide, which contributes to the damage phenotype